

1 **Impacts of climate change and emissions on atmospheric oxidized**
2 **nitrogen deposition over East Asia**

3
4 Junxi Zhang¹, Yang Gao^{2,3*}, L. Ruby Leung⁴, Kun Luo^{1*}, Huan Liu⁵, Jean-Francois Lamarque⁶,

5 Jianren Fan¹, Xiaohong Yao^{2,3}, Huiwang Gao^{2,3} and Tatsuya Nagashima⁷

6
7 ¹State Key Laboratory of Clean Energy, Department of Energy Engineering, Zhejiang
8 University, Hangzhou, Zhejiang, 310027, China

9 ²Key Laboratory of Marine Environment and Ecology, Ministry of Education of China, Ocean
10 University of China, Qingdao, Shandong, 266100, China

11 ³Qingdao National Laboratory for Marine Science and Technology, Qingdao 266100, China

12 ⁴Atmospheric Sciences and Global Change Division, Pacific Northwest National Laboratory,
13 Richland, Washington, 99354, USA

14 ⁵School of Environment, Tsinghua University, Beijing, 100084, China

15 ⁶Atmospheric Chemistry and Climate and Global Dynamics Divisions, National Center for
16 Atmospheric Research, Boulder, Colorado, USA

17 ⁷National Institute for Environmental Studies, Tsukuba, Japan

18
19 *Correspondence to: Dr. Yang Gao (yanggao@ouc.edu.cn)

20 Dr. Kun Luo (zjulk@zju.edu.cn)

Abstract

A multi-model ensemble of Atmospheric Chemistry and Climate Model Intercomparison Project (ACCMIP) simulations are used to study the atmospheric oxidized nitrogen (NO_y) deposition over East Asia under climate and emission changes projected for the future. Both dry and wet NO_y deposition shows significant decreases in the 2100s under RCP 4.5 and RCP 8.5, primarily due to large anthropogenic emission reduction over both land and sea. However, in the near future of the 2030s, both dry and wet NO_y deposition increases significantly due to continued increase in emissions. Marine primary production from both dry and wet NO_y deposition increases by 19-34% in 2030s and decreases by 34-63% in 2100s over the East China Sea. The individual effect of climate or emission changes on dry and wet NO_y deposition is also investigated. The impact of climate change on dry NO_y deposition is relatively minor, but the effect on wet deposition, primarily caused by changes in precipitation, is much higher. For example, over the East China Sea, wet NO_y deposition increases significantly in summer due to climate change by the end of this century under RCP 8.5, which may subsequently enhance marine primary production. Over the coastal seas of China, as the transport of NO_y from land becomes weaker due to the decrease of anthropogenic emissions, the effect of ship emission and lightning emission becomes more important. On average, the seasonal mean contribution of ship emission to total NO_y deposition is projected to be enhanced by 24-48% and 3-37% over Yellow Sea and East China Sea, respectively, by the end of this century. Therefore, continued control of both anthropogenic emission over land and ship emissions may reduce NO_y deposition to the Chinese coastal seas.

Key words: ACCMIP, NO_y deposition, RCP 8.5, ship emission

69 **1. Introduction**

70 As a nutrient, nitrogen is essential to the terrestrial and marine ecosystems and plays
71 vital roles in lives on earth from many perspectives such as human health (Galloway et
72 al., 2008), biodiversity (Butchart et al., 2010), primary production (Doney et al., 2007;
73 Stevens et al., 2015), etc. The oceans comprise the largest and most important
74 ecosystems on Earth and atmospheric nitrogen deposition is an important pathway for
75 delivering nutrients to the ocean (Duce et al., 2008).

76 The characteristics of atmospheric deposition have been widely studied around the
77 world. The concentrations and fluxes of trace elements in atmospheric deposition are
78 influenced by many factors such as rainfall amount, local emissions as well as the long-
79 range transport of pollutants, etc. (Kim et al., 2000; Cong et al., 2010; Theodosi et al.,
80 2010; Vuai and Tokuyama, 2011; Kim et al., 2012; Connan et al., 2013; Montoya-
81 Mayor et al., 2013). Studies have shown significant changes of nitrogen deposition in
82 the future under the influence of changes in both climate and emissions following the
83 representative concentration pathways (RCPs) (Van Vuuren et al., 2011; Ellis et al.,
84 2013; Lamarque et al., 2013a).

85 Since projections of future changes in nitrogen deposition from individual models
86 are prone to specific model errors (Reichler and Kim, 2008; Shindell et al., 2013), multi-
87 model ensembles in either climate (Gao et al., 2014; 2016) or chemistry (Lamarque et
88 al., 2013a; 2013b) are important for identifying robust and non-robust changes
89 projected by models. This study uses the nitrogen deposition from an ensemble of
90 models that contributed to the Atmospheric Chemistry and Climate Model
91 Intercomparison Project (ACCMIP; (Lamarque et al., 2013b)). The nitrogen deposition
92 includes both the oxidized nitrogen deposition (NO_y , mainly including NO , NO_2 , NO_3^- ,
93 N_2O_5 , HNO_3 , HNO_4 and organic nitrates) and reduced nitrogen (NH_x , mainly including
94 NH_3 , NH_4^+ and organic ammonium). Since the number of models with NH_x in ACCMIP
95 is less than 5, this study only focuses on the NO_y (10 models or so) deposition, which
96 mainly results from NO_x emissions.

97 Due to the rapid economic development in China, NO_x emission increase in the past
98 (Wang et al., 2013) has led to an increase of nitrogen deposition. For example, Liu et
99 al. (2013) found that nitrogen deposition over land in China increased from 13.2 kg/ha
100 in 1980s to 21.1 kg ha⁻¹ in 2000s, with increase of 60%. In addition, the increased NO_x
101 emission may also enhance NO_y deposition in Chinese coastal seas, due to the
102 atmospheric and riverine transport of NO_x (Luo et al., 2014). In particular, China has a
103 long coastline of almost 18,000 km in length and over 300 million square kilometer sea
104 areas, with high density population and industries in the coastal provinces. For NO_x
105 emissions over the oceans, shipping emission is the dominant contributor (Dalsøren et
106 al., 2009; Eyring et al., 2010). Lauer et al. (2007) discussed the significant impact of
107 shipping emissions on aerosols such as aerosol nitrate burden, implying potentially
108 subsequent influence on nitrogen deposition. Fan et al. (2016) concluded that 85% of
109 ship emissions took place within 200km of the coastlines, indicating a stronger
110 influence of ship emissions on coastal seas than remote areas. Liu et al. (2016) reported
111 that the shipping NO_x emissions in East Asia increased from 1.08 Tg in 2002 to 2.8 Tg
112 in 2013, accounting for nearly 9% of total NO_x emissions in East Asia and 16.5% of
113 global shipping NO_x emissions. In ACCMIP, the NO_x emission over the ocean mainly
114 comes from the shipping, with much smaller amount from aircraft as well as lightning,
115 since lightning NO_x is concentrated in the tropical land areas (Price et al., 1997).

116 Studies on the changes of nitrogen deposition under the influence of both climate
117 and emission changes have been limited over East Asia. Using the old Special Report
118 on Emissions Scenarios (SRES) such as A2, Lamarque et al. (2005) found large
119 increases of nitrogen deposition over East Asia due to increased emissions, whereas the
120 effect from climate change is much smaller and lacks consensus due to the small
121 ensemble size. In 2100 nitrogen deposition changes due to changes in climate are much
122 less than changes due to increased nitrogen emissions. In contrast, based on the new
123 scenarios RCP 4.5 and 8.5, Lamarque et al. (2013a) found that the total NO_y deposition
124 (wet + dry; Fig. 5a in Lamarque et al. (2013a)) over East Asia was projected to decrease
125 by the end of this century due to the combined effect of emissions and climate, but the
126 changes are mainly triggered by the decrease of emissions. However, the individual

127 effect of climate or emissions was not examined in that study. With the same dataset of
128 ACCMIP, Allen et al. (2015) found that by keeping the emissions at current level,
129 aerosol wet deposition decreases over the land areas of tropics and Northern
130 Hemisphere mid-latitude due to the decrease of large scale precipitation, subsequently
131 enhancing the increase of wet deposition over the ocean through the transport effect.
132 Climate change alone may modulate the changes in the deposition, particularly for wet
133 deposition due to the response of precipitation to climate change. Hence, it is important
134 to elucidate the influence of climate and emission changes on the dry and wet NO_y
135 deposition over East Asia using the multi-model ensemble ACCMIP results.

136 In what follows, we first discuss the capability of ACCMIP in capturing the
137 deposition patterns, followed by the changes of dry and wet deposition in future under
138 the combined effect of climate change and emissions. Lastly, we elucidate the
139 individual effect from climate change or emissions.

140 **2. Model description**

141 In this study, about 10 models from ACCMIP are used, similar to Lamarque et al.
142 (2013b). All the data are interpolated to a spatial resolution of $2^\circ \times 2^\circ$ to facilitate
143 analysis and comparison across models. To evaluate the impacts of climate and
144 emission change as well as to isolate their individual effect, five cases of ACCMIP
145 scenarios are used in this study, as listed in Table 1. The base case over the historical
146 period covers the decade of 2000, mainly from 2001-2010. Two cases target the
147 investigation of both climate and emission changes under future scenarios of RCP 4.5
148 and RCP 8.5, covering two periods in the decades of 2030 and 2100 (first column of
149 Table 1). The remaining two cases are used to investigate the impact from climate
150 change only in the 2030s and 2100s under RCP 8.5 by maintaining emission at the level
151 of year 2000 (last column of Table 1). As different models have different simulation
152 years, some models may not cover the entire decades of 2030 and 2100. Detailed
153 simulation lengths for each model are listed in Table S1. In the ACCMIP dataset, the

154 summation of all simulated oxidized nitrogen species is referred to as NO_y, which is the
 155 major focus of this study.

156 Table 1. Scenarios used in this study

157

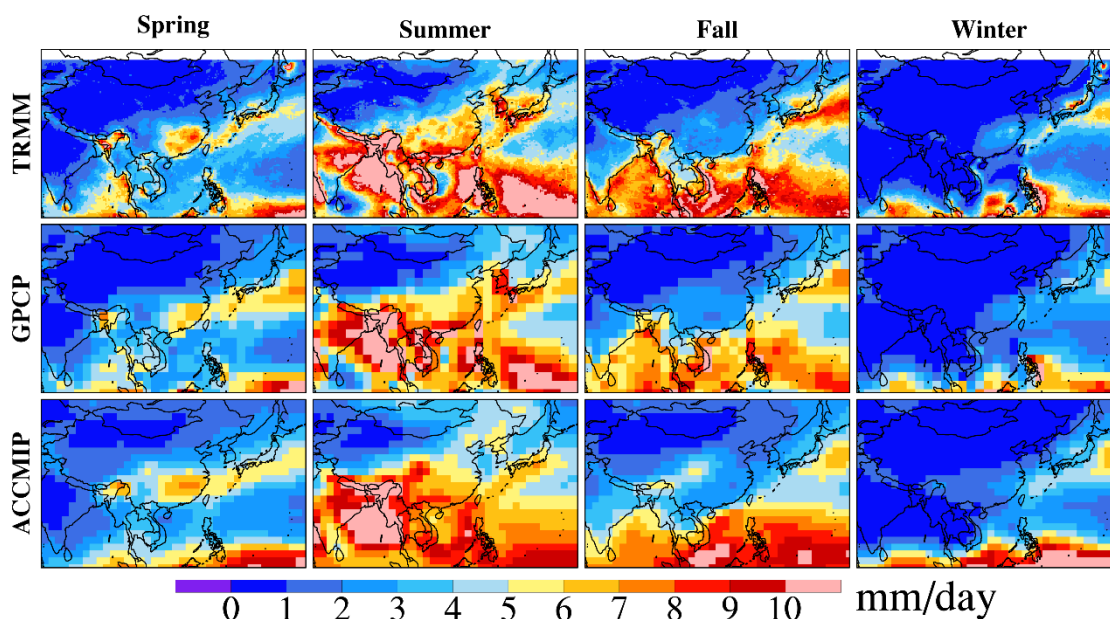
	Base	Changes in both climate and emissions		Climate change only	
Scenarios	Historical	RCP 4.5	RCP 8.5	Em2000Cl2030	Em2000Cl2100
Period	2000-2010	2030-2039	2030-2039	2030-2039	2100-2109
		2100-2109	2100-2109		

158

159 **3. Evaluation of the ACCMIP results**

160 The deposition results of ACCMIP have been extensively evaluated previously
 161 across land areas by comparing with three datasets including North American
 162 Deposition Program (NADP), European Monitoring and Evaluation Programme
 163 (EMEP) and Acid Deposition Monitoring Network in East Asia (EANET), and
 164 reasonable performance was demonstrated by the ACCMIP results (Lamarque et al.,
 165 2013a). There is a lack of deposition data over the ocean, making evaluation of the
 166 ACCMIP results across the oceans difficult. Recently, Baker et al. (2017) conducted an
 167 intensive evaluation of the ACCMIP multi-model mean based on a large number of dry
 168 NO_y deposition samples, i.e., a total of 770 samples collected over the Pacific, showing
 169 comparable spatial distributions between observations and ACCMIP, such as a
 170 consistent northwest-southeast gradient with higher deposition flux closer to the coast
 171 (Fig. 12 in Baker et al. (2017)). In terms of wet deposition, considering the close
 172 relationship between wet deposition and precipitation (Kryza et al., 2012; Wałaszek et
 173 al., 2013), evaluation of precipitation is performed using the Tropical Rainfall
 174 Measuring Mission (TRMM; <http://pmm.nasa.gov/trmm>) and Global Precipitation
 175 Climatology Project (GPCP) v 2.3 (Adler et al., 2018) precipitation data. Fig. 1 shows
 176 a comparison of the annual mean precipitation over the historical period (2000-2010)
 177 among the ACCMIP multi-model ensemble mean and TRMM, which only covers
 178 60°N-60°S, and GPCP. In general, the ACCMIP mean precipitation well captures the

179 spatial variations of the observed precipitation from both TRMM and GPCP, with
 180 stronger precipitation in the southern part of Asia, particularly over the South China Sea
 181 and the Bay of Bengal, and lighter precipitation in northern China (i.e., Northwest
 182 China). In particular, the rain belt stretching from the east of Japan to the Philippines in
 183 summer is also well captured by ACCMIP. To further illustrate the uncertainties among
 184 different models, the standard deviation of seasonal mean precipitation across all
 185 ACCMIP models over East Asia is shown in Fig. S1, within 1-2 mm/day over Chinese
 186 coastal seas.



187
 188 Fig. 1. Evaluation of seasonal mean precipitation during 2001-2010: ACCMIP multi-model
 189 ensemble mean vs. TRMM and GPCP

190 4. Future changes of NO_y deposition in East Asia

191 Considering the uncertainty and variability among multiple ACCMIP results, all
 192 analyses, i.e., the future changes of deposition, are performed based on model
 193 agreement and statistical significance. Following our previous studies (Gao et al., 2014;
 194 2015), results at a model grid cell are considered to have agreement if at least 70% of
 195 the ACCMIP models show the same sign of change as the ACCMIP multi-model
 196 ensemble mean. For models showing agreement with the ensemble mean, if more than
 197 half of the models show statistical significance at 95% level, then the ensemble mean

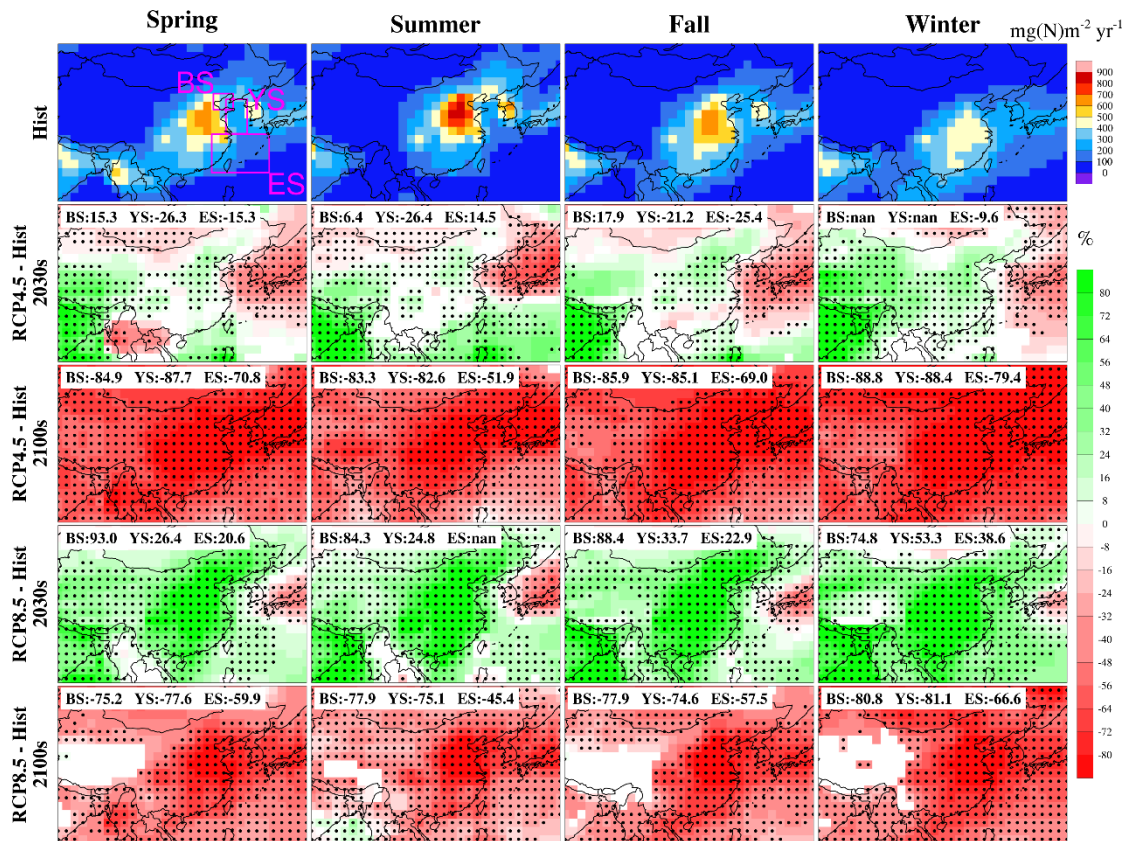
198 change for that particular grid is considered to be statistically significant.

199 The seasonal mean distribution of dry NO_y deposition over East Asia areas for
200 historical (2001-2010) and projected future changes under RCPs scenarios (RCP 4.5
201 and RCP 8.5) during the two periods of 2030 and 2100 are shown in Fig. 2. The four
202 seasons defined in this study are spring (March to May), summer (June to August), fall
203 (September to November) and winter (December to February). Regional mean changes
204 over BYE areas are shown in each panel, calculated from multi-model mean results.
205 The corresponding standard deviations of multiple models are shown in Table S2.

206 As anthropogenic activities play important roles in NO_x emissions, high
207 atmospheric dry nitrogen (NO_y) deposition values mainly cluster around areas with high
208 population density and industrial activities in the historical periods (top row of Fig. 2),
209 e.g., high values of NO_y deposition can be seen in East China, Korea, Japan and their
210 coastal seas. In this study, in addition to the land areas, we also focus on three coastal
211 seas in East Asia (Bohai Sea, Yellow Sea and East China Sea from high latitude to low
212 latitude, referred to as the BYE areas below), marked by the three black boxes in Fig.
213 2a. A gradient of decreasing NO_y deposition is found (top row of Fig. 2) from eastern
214 China to the coastal areas. Seasonal variations show that over mainland China, summer
215 is the season with the highest dry and wet NO_y deposition, with high dry deposition
216 likely caused by the high deposition velocity (Zhang et al., 2017) and wet deposition
217 due to larger precipitation in summer, consistent with previous studies (Liu et al., 2017;
218 Zhang et al., 2017; Xu et al., 2018). Over the ocean such as Yellow Sea and East China
219 Sea, the notably higher NO_y deposition (first row of Fig. 2) is partly attributed to NO_x
220 emission transported from land to the coastal seas. In particular, the dry NO_y deposition
221 over the East China Sea is obviously higher in winter compared to summer, likely
222 resulting from enhanced transport by the northwesterly winds during the winter
223 monsoon (Ding, 1991).

224 Considering the projected future changes of NO_y deposition, we show the
225 distributions in the 2030s and 2100s under the RCP 4.5 and RCP 8.5 scenarios,
226 representing near-term and long-term changes. Dry NO_y deposition decreases
227 remarkably in the 2100s under the RCP 4.5 and RCP 8.5 scenarios over East Asia, a

228 result of large decrease in emissions (second column in Fig. S2 in the supporting
 229 information). In the 2030s, besides the decrease of dry deposition in Japan, Korea and
 230 the surrounding areas, RCP 8.5 shows a predominant increase of dry deposition (Fourth
 231 row in Fig. 2); in contrast, robust significant increases in western China and India are
 232 projected, with little or weak signals in eastern China in RCP 4.5, consistent with the
 233 emission change patterns (first column in Fig. S2).
 234



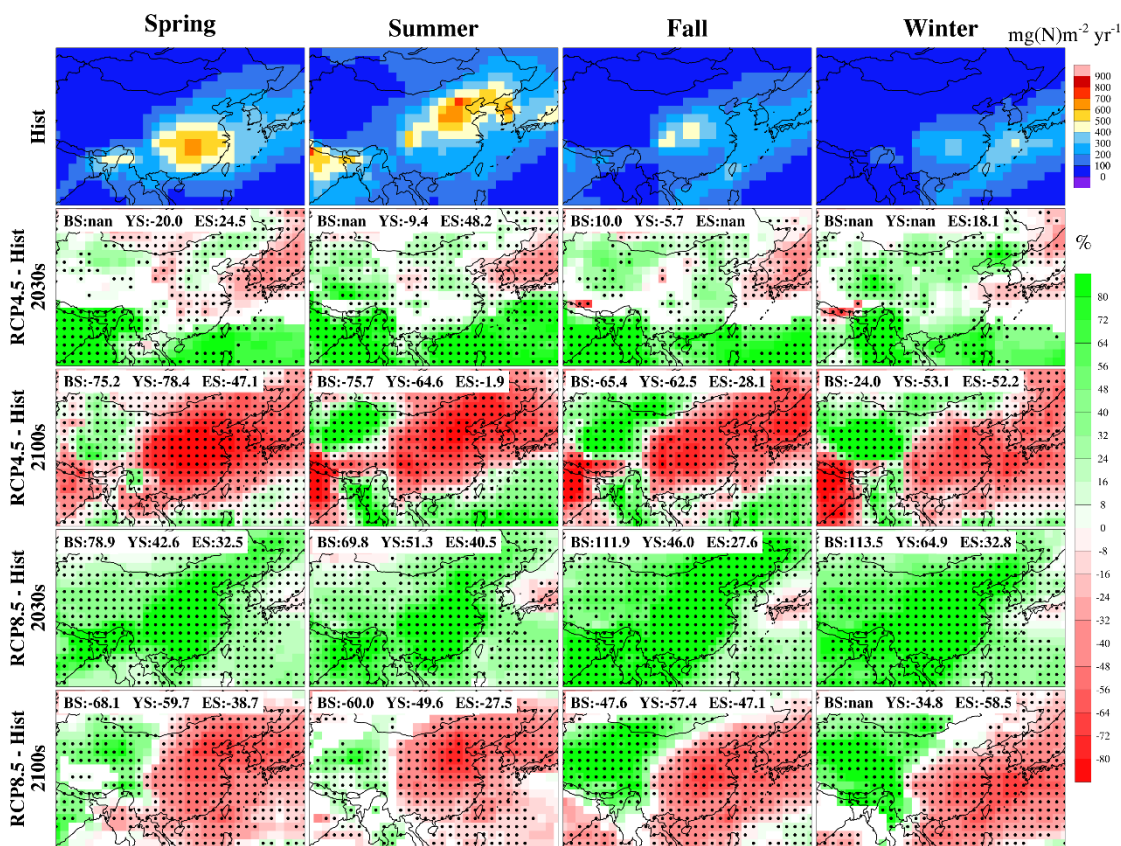
235
 236 Fig. 2 Spatial distribution of mean seasonal dry NO_y deposition over East Asia under historical
 237 (2001-2010; top row) as well as the future changes (second to fifth rows representing changes under
 238 RCP 4.5 2030, RCP 4.5 2100, RCP 8.5 2030 and RCP 8.5 2100 in relative to historical period). Only
 239 grids with multi-model agreement are shown (grids without model agreement are in white), and
 240 stippling marks areas with statistical significance ($\alpha=0.05$). Regions of Bohai Sea (BS), Yellow Sea
 241 (YS) and East China Sea (ES) are marked by the pink rectangles in the top left panel, with mean
 242 changes shown on the top left of each panel starting from the second row. Only grids with significant
 243 change in the ocean areas are calculated. The mean change of a region is set to nan if the number of
 244 significant grids in this region is less than half of the area.

245

246 For wet NO_y deposition, as discussed earlier, summer is the season with strongest
 247 deposition (first row of Fig. 3), primarily caused by the largest precipitation among the

248 four seasons (Fig. 1). In the 2030s, changes of wet deposition (second and fourth rows
 249 of Fig. 3) are in general similar to the patterns of dry deposition changes (second and
 250 fourth rows of Fig. 2), with standard deviation of wet deposition shown in Table S3. In
 251 the 2100s, the patterns of wet deposition changes are different from those of dry
 252 depositions, with relatively clear east/west dipole features in particular under RCP 8.5.
 253 To elucidate what controls the dipole patterns, the individual effect of climate change
 254 and emissions is discussed in the next section.

255



256

257

Fig. 3. Same as Fig. 2 except for wet NO_y deposition.

258

5. The impact of climate change or emissions on NO_y deposition

259

Two scenarios from ACCMIP are used in this study to isolate the influence of
 260 anthropogenic emissions and climate change on NO_y deposition. The two scenarios are
 261 shown in Table 1, with emissions kept at the current level (the decade of 2000) but
 262 climate for the 2030s and 2100s under RCP 8.5 are compared.

263 Climate change alone has negligible contributions to the dry NO_y deposition
264 changes, as shown in Fig. 4. Generally, calculation of dry deposition flux in chemical
265 models follows equation 5.1, where F is vertical dry deposition flux, C is concentration
266 of specific gas or particle and v_d is the dry deposition velocity.

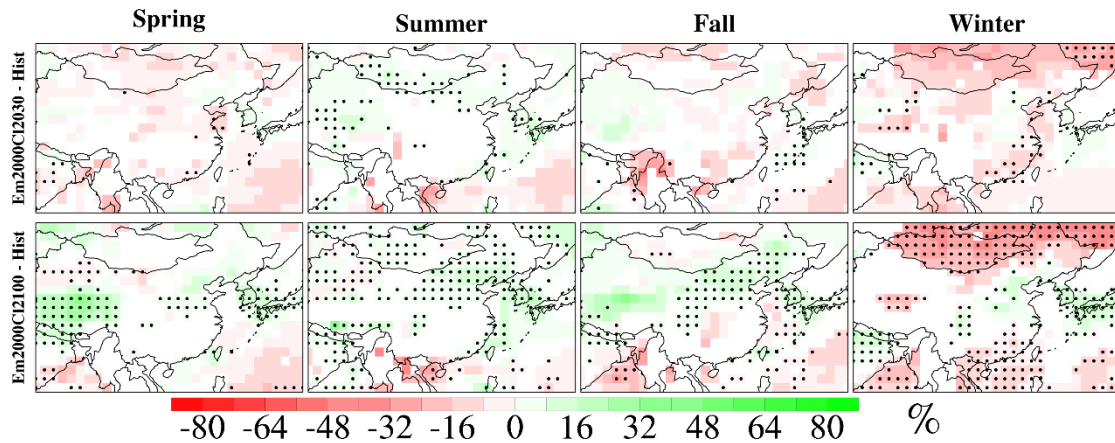
$$267 \quad F = -v_d C \quad (5.1)$$

268 All models in ACCMIP calculated dry deposition velocity using the resistance
269 approach (Lamarque et al., 2013b), which defines the inverse of dry deposition velocity
270 as equation 5.2,

$$271 \quad \frac{1}{v_d} = r_t = r_a + r_b + r_c \quad (5.2)$$

272 where r_t is the total resistance, r_a is the aerodynamic resistance which is common to
273 all gases, r_b is the quasilaminar sublayer resistance and r_c is the bulk surface resistance
274 (Steinfeld, 1998). As r_b depends on the molecular properties of the target substance and
275 deposition surface and r_c depends on the nature of surface (Steinfeld, 1998), they do not
276 vary under climate change. As for r_a, it plays a significant role in transporting gases and
277 particles from atmosphere to the receptor surface. R_a is governed by atmospheric
278 turbulent transport, mainly controlled by the wind shear as well as buoyancy (Erisman
279 and Draaijers, 2003). Therefore, climate change affects dry deposition velocity for the
280 gases or particles mainly through its modulation of r_a. As shown in Fig. 4, the changes
281 of dry depositions from climate change alone are mostly negligible compared to the
282 total changes from both climate change and emissions (Fig. 2), indicating statistically
283 insignificant change of r_a under a warmer climate.

284



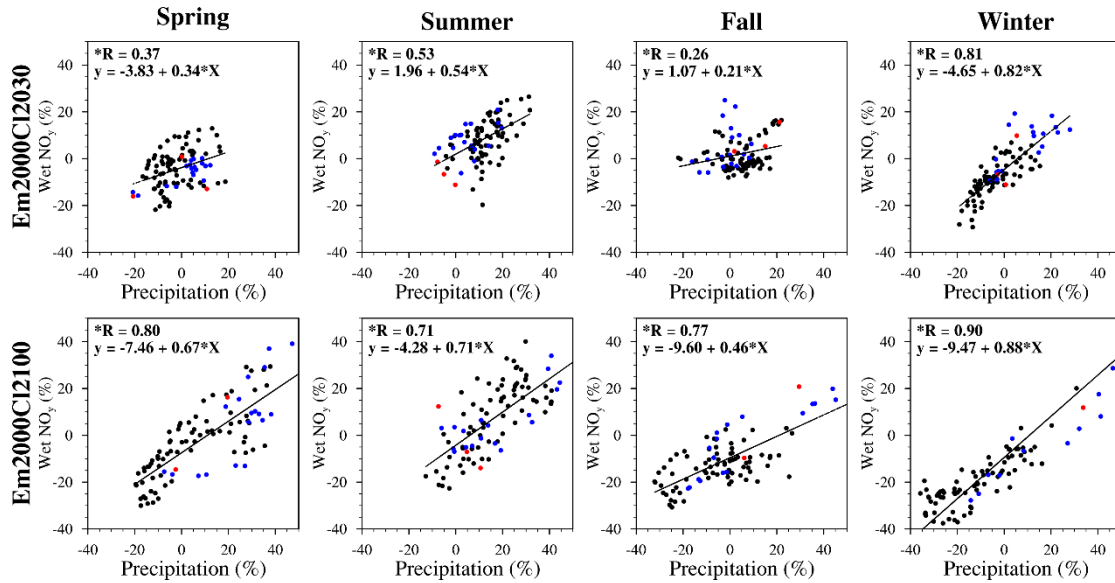
285

286 Fig. 4. Spatial distribution of mean seasonal dry NO_y deposition change over East Asia under
 287 experimental scenarios of ACCMIP (Em2000Cl2030 and Em2000Cl2100) relative to historical
 288 period (2001-2010). The distribution of mean seasonal dry NO_y deposition under historical
 289 period is shown in Fig. 2 (top row). Only grids with multi-model agreement are shown (grids without model
 290 agreement are in white), and among the grids with model agreement, stippling marks statistical
 291 significance ($\alpha=0.05$).

292

293 Considering the impact of climate conditions on NO_y deposition, precipitation is an
 294 important factor and has been shown to positively correlate with wet NO_y deposition
 295 (Kryza et al., 2012; Wałaszek et al., 2013). In order to further quantify the relationship
 296 between wet deposition and precipitation, we display in Fig. 5 the correlation between
 297 the changes of precipitation and wet NO_y deposition over the BYE areas for the
 298 scenarios with fixed emissions. All correlations are positive and statistically significant.
 299 There is a larger inter-model spread of changes in Em2000Cl2100 compared to
 300 Em2000Cl2030, and the larger changes in precipitation and wet deposition allow a
 301 stronger correlation between them to emerge in the 2100s relative to the 2030s.
 302 Meanwhile, winter owns the highest correlation in both Em2000Cl2030 and
 303 Em2000Cl2100, partly related to the significant decrease of both wet NO_y deposition
 304 and precipitation in winter under Em2000Cl2100 over East China Sea which will be
 305 discussed in detail next.

306

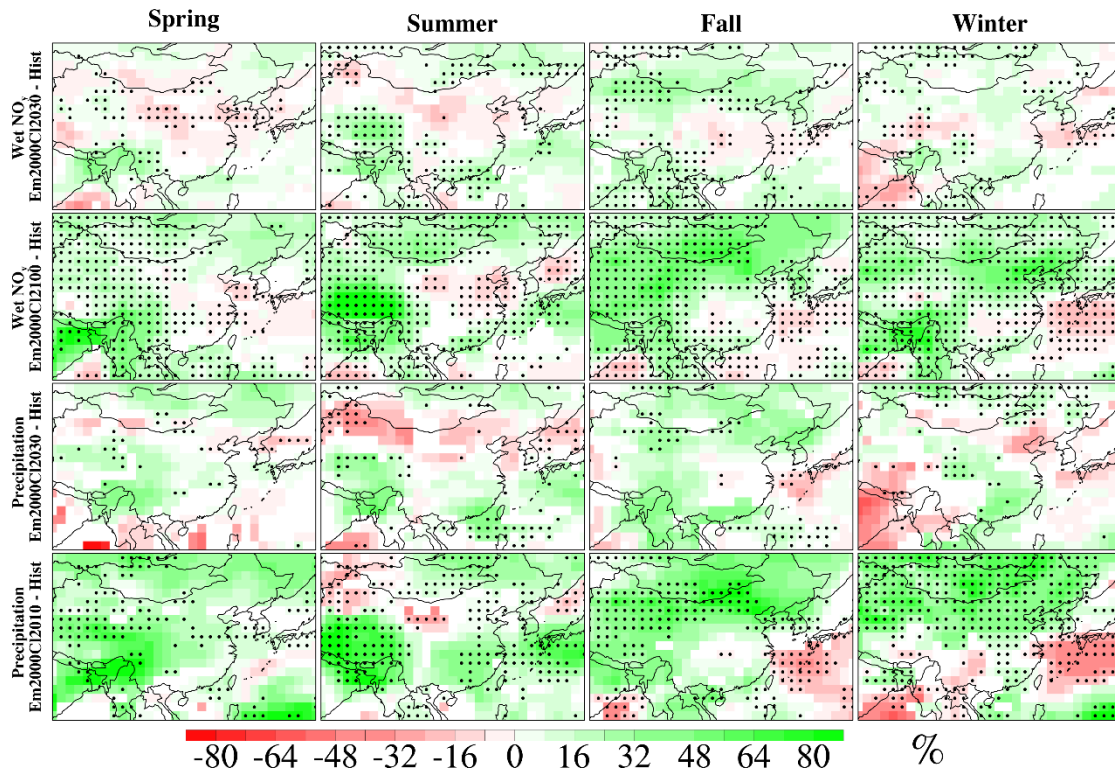


307

308 Fig. 5. Comparison between precipitation and wet NO_y deposition changes under the experimental
 309 scenarios of ACCMIP (Em2000CI2030 and Em2000CI2100) relative to historical period (2001-
 310 2010) over Bohai Sea (red points), Yellow Sea (blue points) and East China Sea (black points). An
 311 r-test ($\alpha=0.05$) is performed in each panel for statistical significance and the star before “R” indicates
 312 statistical significance at 95% confidence level. Each point in this figure corresponds to the results
 313 from an individual model of ACCMIP.

314

315 As depicted in Fig. 6, the changes of wet deposition in the 2030s due to climate
 316 change are mostly insignificant (first row) and correspond well with the insignificant
 317 changes of precipitation (third row). Similarly, the patterns in the 2100s between the
 318 changes of wet deposition (second row) and precipitation (fourth row) are quite
 319 consistent. For example, in spring, summer and fall, a dominant increase in western
 320 China is projected (first three panels in the second and fourth rows), whereas in winter,
 321 a north and southeastern dipole feature is clearly seen. Over the East China Sea, wet
 322 NO_y deposition increases significantly in summer (18%) and decreases significantly in
 323 winter (-13%), indicating a remarkable influence of climate change on the wet NO_y
 324 deposition. The changes of precipitation are generally consistent with that reported in
 325 other studies. Both Chong-Hai and Ying (2012) and Wang and Chen (2014) show
 326 significant increase of precipitation except for eastern South China at the end of the 21st
 327 century under RCP 8.5. Comparing Fig. 6 with Fig. 3, it is clear that the dipole pattern
 328 of changes in wet deposition in the 2100s shown in Fig. 3 is primarily related to the
 329 large reduction of emission over eastern China.



330

331 Fig. 6. Spatial distribution of mean seasonal wet NO_y deposition change and precipitation change
 332 under EM2000CI2030 and Em2000CI2100 relative to historical period (2001-2010). The panels are
 333 drawn and arranged in the same manner as Fig. 2.

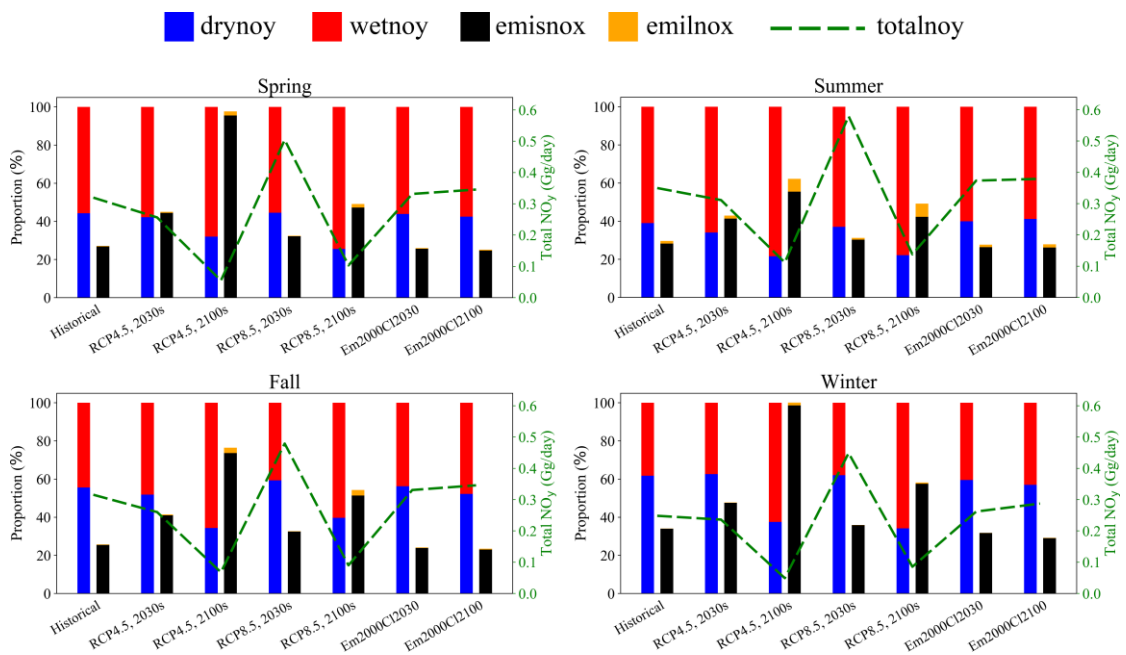
334

335 From the global perspective, the emission of nitrogen oxide is in general balanced
 336 by the NO_y deposition as documented in Lamarque et al. (2013a) using the ACCMIP
 337 model results, although NO_y deposition might be larger due to the downward transport
 338 from the stratosphere. For a particular region, the NO_y deposition can be considered as
 339 the contribution of both local NO_x emission such as shipping and lightning as well as
 340 the transport such as from the East Asia continent. Therefore, we calculate the multi-
 341 model seasonal mean NO_y deposition and NO_x emissions from shipping and lightning.
 342 As was documented by Liu et al. (2016), ship emissions from East China Sea may
 343 account for a large percentage (31%) of the total ship emission in East Asia, indicating
 344 the strong effect of ship emission over Chinese coastal seas. To avoid biases from spatial
 345 interpolation, calculation is performed based on the original model grid and regionally
 346 averaged for each model. Since the changes in Bohai are less significant in general,
 347 particularly in the near future (second row of Figs. 2,3), we only focus on the emission
 348 and deposition changes over Yellow Sea and East China Sea. Summary of shipping and

349 lightning NO_x emission over Yellow Sea and East China Sea under historical, RCP and
350 other scenarios is listed in Table S4. Overall, lightning emission is much smaller than
351 shipping emission. In future, seasonal mean shipping emission increases in 2030s in
352 particular under RCP 8.5 and decreases in 2100s under both RCP scenarios, whereas
353 the changes of lightning emission are small except in summer with mean increase of
354 73% over Yellow Sea and East China Sea. Based on NO_x emission and NO_y deposition,
355 the percentage of dry and wet deposition, as well as the ratio of ship emission and
356 lightning emission to the total NO_y deposition are shown in Figs. 7 and 8. The ratio of
357 ship emission and lightning emission to the total NO_y deposition is used to characterize
358 their contribution to NO_y deposition with the assumption that all ship and lightning
359 emission contribute to the NO_y deposition, which can be considered an upper bound of
360 their contribution.

361 A couple of features can be identified from Fig. 7 and Fig. 8. First, total NO_y
362 deposition was shown as the green dash line, with all values consistent with the spatial
363 distributions in Figs. 2-4. By the end of this century (2100), total NO_y deposition
364 decrease substantially under both RCP 4.5 and RCP 8.5, whereas in 2030s, total
365 deposition shows dramatic increase in RCP 8.5, but moderate change in RCP 4.5 (slight
366 decrease in Yellow sea and increase in East China sea). The percentage of dry deposition
367 over Yellow Sea and East China Sea (third and fifth blue color bars from the left in each
368 panel of Figs. 7, 8) decreases in the 2100s under RCP 4.5 and RCP 8.5, consistent with
369 the patterns shown in Fig. 2 and Fig. 3 (third and fifth rows), due primarily to emission
370 reduction. Second, albeit the decrease of shipping emission in 2100s, the contribution
371 of ship emission to total NO_y deposition increases substantially under both RCP 4.5
372 and 8.5 over Yellow Sea and East China Sea (black color bars in Figs. 7,8), due
373 primarily to the larger emission reduction over land (e.g., eastern China) compared to
374 ocean (Fig. S2). For instance, over the historical period, the seasonal contribution of
375 ship emission to total NO_y deposition is 22%-30% and 52%-82% for Yellow Sea and
376 East China Sea, respectively; however, in 2100, it reaches 56%-99% (RCP 4.5) and 42-
377 58% (RCP 8.5) for Yellow Sea, 81% to almost 100% (RCP 4.5) and 74% to almost 100%
378 (RCP 8.5) for East China Sea, with mean seasonal increase of 24-48% and 3%-37% for

379 Yellow Sea and East China Sea, respectively. Third, the contribution of lightning NO_x
 380 in spring and winter is negligible, however, the contribution is nontrivial in summer and
 381 fall (orange bars in Figs. 7,8). In particular, due to the reduction in anthropogenic
 382 emissions over land and ship emissions in 2100s under RCP 4.5 and RCP 8.5 (Fig. S2)
 383 along with the increase of lightning NO_x emissions over Chinese coastal seas (Table
 384 S4), the contribution of lightning NO_x becomes more obvious compared with the case
 385 without emission reduction. For example, in the summer of the 2100s, the contribution
 386 of lightning NO_x increases from 1% to 7% (both RCP 4.5 and RCP 8.5) over Yellow
 387 Sea, 3% to 7% in RCP 4.5 and 6% in RCP 8.5 over East China Sea. In the fall of the
 388 2100s, the contribution of lightning NO_x increases from less than 1% to 3% (both RCP
 389 4.5 and RCP 8.5) over Yellow Sea, and 1% to 4% (both RCP 4.5 and RCP 8.5) in East
 390 China Sea. These results illustrate a shift in the future towards enhanced impacts from
 391 ship and lightning emissions when anthropogenic emissions are largely controlled in
 392 the upwind land regions.
 393



394
 395 Fig. 7. Stacked bars of seasonal ratio of NO_y deposition from wet (wetnoy) and dry (drynoy)
 396 deposition and NO_x emissions from ship (emisnox) and lightning (emilnox) to the total (wet + dry)
 397 NO_y deposition in the historical and RCP scenarios over Yellow Sea. Two color bars are shown for
 398 each period with the left one representing dry NO_y (blue) and wet NO_y (red) deposition and the right
 399 one representing emisnox (black) and emilnox (orange). A green dash line representing total NO_y
 400 deposition is added for each panel with y-axis on the right.

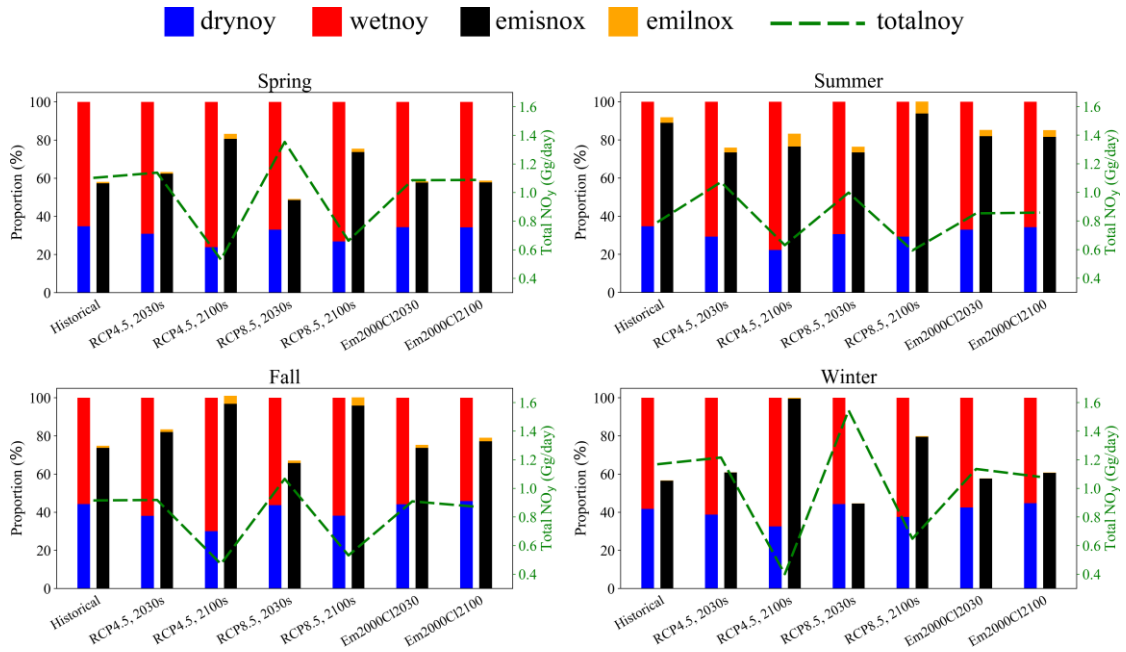


Fig. 8 Same as Fig. 7 except for East China Sea.

6. Marine primary production over the BYE areas and its future change

Generally, the Chinese coastal seas have rich nutrients and high total primary production (Gong et al., 2000; Son et al., 2005). Thus, these areas seldom lack nutrient but sometimes eutrophication is an environmental issue. For instance, a massive *Ulva prolifera* bloom occurred in June 2008 in the Yellow Sea and the harmful algal bloom caught a lot of attention. Hu et al. (2010) found that algal blooms occur in each summer of 2000-2009 in the Yellow Sea and East China Sea. Atmospheric deposition is an important source of nutrient for the marine ecosystem, and it can facilitate primary production (PP) in the ocean surface and contribute to the development of harmful algal blooms (Paerl and Hans, 1997; Paerl et al., 2002).

Several previous studies have investigated PP over the BYE areas and estimated the historical annual PPs to be $97\text{gC m}^{-2}\text{ yr}^{-1}$, $236\text{gC m}^{-2}\text{ yr}^{-1}$ and $145\text{gC m}^{-2}\text{ yr}^{-1}$, respectively, for Bohai Sea, Yellow Sea and East China Sea (Guan et al., 2005; Gong et al., 2003). In this study, based on the assumption that all NO_y deposited into surface ocean can be absorbed by phytoplankton, we estimate the model averaged PP from NO_y

419 deposition in the historical period over the BYE areas according to the Redfield ratio
420 (Tett et al., 1985). The Redfield ratio refers to the ratios of carbon, nitrogen and
421 phosphorus in phytoplankton listed in equation 6.1. Equation 6.2 are used to calculate
422 PP generated from NO_y deposition, where PP_{noy} represents the PP from NO_y
423 deposition and NO_y represents total NO_y (wet + dry) deposition.

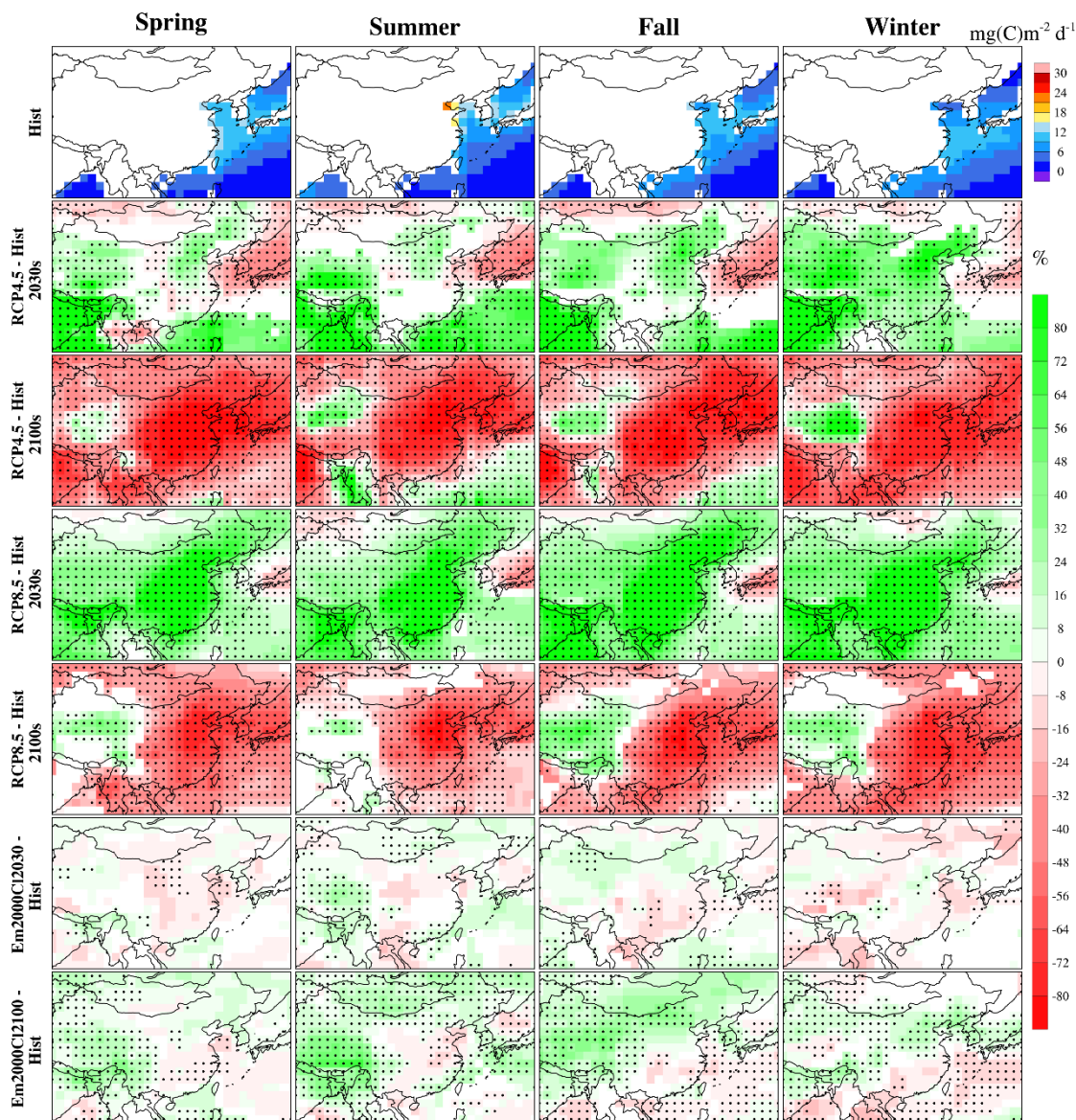
$$424 \quad C : N : P = 106 : 16 : 1 \quad (6.1)$$

$$425 \quad \text{PP}_{\text{noy}} = \text{NO}_y \times \frac{106}{16} \quad (6.2)$$

426 Results show that PP from historical NO_y deposition is 5, 5.4 and 4.4 $\text{gC m}^{-2} \text{yr}^{-1}$
427 over Bohai Sea, Yellow Sea and East China Sea, accounting for 5%, 2% and 3% of PP
428 in those three seas, respectively. These values are consistent, albeit of slightly smaller
429 due to the consideration of oxidized nitrogen only in our study, with previous studies.
430 For instance, Qi et al. (2013) indicated a contribution of 0.3~6.7% to PP from total
431 dissolved nitrogen deposition over the Yellow Sea from July 2005 to March 2006, and
432 Zhang et al. (2010) found that total inorganic nitrogen deposition accounted for 1.1~3.9%
433 of PP over East China Sea in 2004.

434 Recently, several studies have evaluated the change of global primary production
435 under future climate change (Steinacher et al., 2010; Koga et al., 2011; Laufkötter et al.,
436 2015; Cabré et al., 2015). For instance, based on multi-model ensembles, Cabré et al.
437 (2015) found a general global decrease (up to 30%) of total PP projected under RCP 8.5
438 by the end of this century. We calculate the seasonal PP from NO_y using ACCMIP, with
439 results shown in Fig. 9. It should be noticed that panels from the second row in Fig. 9
440 refer to the percentage changes of total NO_y deposition. According to the Redfield ratio,
441 PP from NO_y is proportional to total NO_y deposition, yielding the same percentage
442 change between PP and NO_y . Therefore, the values in the ocean (Fig. 9) also represent
443 the changes of primary production resulted from NO_y deposition. Note that PP in the
444 first row of Fig. 9 is the equivalent primary production converted from NO_y deposited
445 into the ocean through nutrients uptake by phytoplankton. Due to low sea surface
446 temperature in winter, the conversion can hardly happen and the nutrients may remain
447 until spring (Reay et al., 1999). Therefore, actual PP from NO_y may shift from winter

448 to spring instead. Moreover, as the Redfield ratio is used to estimate PP from NO_y under
449 all scenarios, potential influence of changes in other nutrients (e.g., carbon and
450 phosphorus) under RCP scenarios and experimental scenarios is not considered. Under
451 RCP scenarios, consistent with the change patterns of total NO_y deposition (not shown),
452 PP from NO_y decreases significantly over the BYE areas in the 2100s, by 60~68% and
453 34~63% in the four seasons over the Yellow Sea and East China Sea, respectively, under
454 RCP 8.5 (third and fifth rows in Fig. 9). However, in the 2030s, PP from NO_y shows an
455 increase over the BYE areas under RCP 8.5 (e.g., 32~53% in the Yellow Sea and 19~34%
456 in East China Sea; fourth row in Fig. 9), with smaller increase or decrease under RCP
457 4.5 (second row in Fig. 9). The large increase of NO_y in the near future suggests the
458 increased risk of algal blooms if emission continues to increase, and the reduction in
459 NO_y in 2100 indicates the importance of emission reduction in the long-term. Without
460 emission reduction, PP from NO_y is projected to increase in 2100 during summer (last
461 row in Fig. 9) over the East China Sea, consistent with the wet deposition pattern change
462 depicted in Fig. 6, indicating that climate change increases eutrophication through
463 enhancement of precipitation that increases wet deposition over this region. Hence our
464 results illustrate the importance of reducing emissions on PP in the BYE areas in the
465 future.



466
 467 Fig. 9. First row is spatial distribution of marine primary production resulted from NO_y deposition
 468 over East Asia in historical periods. Areas over land are blank because the Redfield ratio is only
 469 applied to the ocean areas. The spatial distributions from the second row refer to the percentage
 470 change of total NO_y deposition for all RCP scenarios and other scenarios used in this study. Values
 471 in the ocean areas can be seen as changes of PP from NO_y based on the definition of the Redfield
 472 ratio. From the second row, all distributions are percentage change compared to historical period
 473 and only values with agreement are shown. Values with statistical significance ($\alpha=0.05$) are marked
 474 with a black dot.
 475

476 7. Conclusions and discussions

477 Atmospheric NO_y deposition over East Asia is analyzed to delineate the influence
 478 of climate and emission changes based on the ACCMIP multi-model ensemble. Under

479 both RCP 4.5 and RCP 8.5 scenarios with combined effect of climate and emission
480 changes, both dry and wet NO_y deposition shows significant decreases in the 2100s,
481 primarily as a result of large reduction in anthropogenic emissions. In the 2030s, both
482 the dry and wet NO_y deposition increases significantly, particularly under RCP 8.5,
483 mainly because of enhanced emissions. The individual effect of climate change and
484 emissions on the dry and wet NO_y deposition is also identified, showing relatively
485 minor impact of climate change on dry NO_y deposition. In terms of wet deposition, the
486 spatial patterns are in general consistent with those in the changes of precipitation,
487 particularly at the end of this century. Take the East China Sea as an example, wet NO_y
488 deposition increases significantly in summer (18%) and decreases significantly in
489 winter (-13%). While climate change alone generally increases wet deposition,
490 reduction of emission has a dominant influence of reducing wet deposition over East
491 China.

492 Over the Chinese coastal seas such as Yellow Sea and East China Sea, with
493 decreasing transport of NO_x from mainland China due to emission reduction, ship and
494 lightning emissions from the ocean become the major source of NO_y deposition, with
495 mean seasonal increase of 24-48% and 3%-37% for Yellow Sea and East China Sea,
496 respectively. Therefore, reducing ship emission in the Chinese coastal areas is a key
497 factor to reduce nitrogen deposition in the future.

498 In the 2030s, PP from NO_y shows increases over the BYE areas under RCP 8.5,
499 suggesting the increased risk of algal blooms if emission such as from ships continues
500 to increase in the near future (Liu et al., 2016). With climate change only, PP from NO_y
501 is projected to increase in 2100 during summer over the East China Sea, indicating a
502 supportive role of climate change on eutrophication, and hence the importance of
503 emission controls.

504 Although the ACCMIP multi-model ensemble has provided valuable information
505 for projecting future changes in NO_y deposition, the models used in ACCMIP have
506 relatively coarse spatial resolution for resolving the complex meteorological and
507 chemical processes. Dynamical downscaling may be applied in the future to further
508 investigate the impact of climate and emission on nitrogen deposition over East Asia

509 and the detailed processes involved. For analysis of marine primary production, we
510 used a very simple approach that ignores biogeochemical processes in the ocean. An
511 ocean biogeochemistry model will be useful to further quantify the effect of climate and
512 emissions on PP.

513

514

515 **Competing interests.** The authors declare that they have no conflict of interest.

516 **Acknowledgement.** This research was supported by grants from the National Key Project of
517 MOST (2017YFC1404101), Shandong Provincial Natural Science Foundation, China
518 (ZR2017MD026) and National Natural Science Foundation of China (41705124, 41822505 and
519 91544110). PNNL is operated for DOE by Battelle Memorial Institute under contract DE-AC05-
520 76RL01830.

521

522 **References:**

523 Adler, R. F., Sapiano, M. R. P., Huffman, G. J., Wang, J. J., Gu, G., Bolvin, D., Long, C., Schneider, U.,
524 Becker, A., and Nelkin, E.: The Global Precipitation Climatology Project (GPCP) Monthly Analysis
525 (New Version 2.3) and a Review of 2017 Global Precipitation, *Atmosphere*, 9, 138, 2018.

526 Allen, R. J., Landuyt, W., and Rumbold, S. T.: An increase in aerosol burden and radiative effects in a
527 warmer world, *Nat. Clim. Change*, 6, 2015.

528 Baker, A. R., Kanakidou, M., Altieri, K. E., Daskalakis, N., Okin, G. S., Myriokefalitakis, S., Dentener,
529 F., Uematsu, M., Sarin, M. M., and Duce, R. A.: Observation- and Model-Based Estimates of
530 Particulate Dry Nitrogen Deposition to the Oceans, *Atmos. Chem. Phys.*, 17, 8189-8210, 2017.

531 Butchart, S. H. M., Walpole, M., Collen, B., Strien, A. v., Scharlemann, J. P. W., Almond, R. E. A., Baillie,
532 J. E. M., Bomhard, B., Brown, C., and Bruno, J.: Global biodiversity: indicators of recent declines,
533 *Science*, 328, 1164-1168, 2010.

534 Cabré, A., Marinov, I., and Leung, S.: Consistent global responses of marine ecosystems to future climate
535 change across the IPCC AR5 earth system models, *Clim. Dynam.*, 45, 1-28, 2015.

536 Chong-Hai, and Ying: The Projection of Temperature and Precipitation over China under RCP Scenarios
537 using a CMIP5 Multi-Model Ensemble, *Atmos. Ocean. Sci. Lib.*, 5, 527-533, 2012.

538 Cong, Z. Y., Kang, S. C., Zhang, Y. L., and Li, X. D.: Atmospheric wet deposition of trace elements to
539 central Tibetan Plateau, *Appl. Geochem.*, 25, 1415-1421,

540 <https://doi.org/10.1016/j.apgeochem.2010.06.011>, 2010.

541 Connan, O., Maro, D., Hebert, D., Rounsard, P., Goujon, R., Letellier, B., and Le Cavelier, S.: Wet and
542 dry deposition of particles associated metals (Cd, Pb, Zn, Ni, Hg) in a rural wetland site, Marais
543 Vernier, France, *Atmos. Environ.*, 67, 394-403, <https://doi.org/10.1016/j.atmosenv.2012.11.029>,
544 2013.

545 Dalsøren, S. B., Eide, M. S., Endresen, and Mjelde, A.: Update on emissions and environmental impacts
546 from the international fleet of ships. The contribution from major ship types and ports, *Atmos. Chem.*
547 *Phys.*, 9, 18323-18384, 2009.

548 Ding, Y. H.: Monsoons over China, *Atmos.sci.library*, 419, 252-252, 1991.

549 Doney, S. C., Mahowald, N., Lima, I., Feely, R. A., Mackenzie, F. T., Lamarque, J.-F., and Rasch, P. J.:
550 Impact of anthropogenic atmospheric nitrogen and sulfur deposition on ocean acidification and the
551 inorganic carbon system, *P. Natl. Acad. Sci.*, 104, 14580-14585, 2007.

552 Duce, R. A., LaRoche, J., Altieri, K., Arrigo, K. R., Baker, A. R., Capone, D. G., Cornell, S., Dentener,
553 F., Galloway, J., Ganeshram, R. S., Geider, R. J., Jickells, T., Kuypers, M. M., Langlois, R., Liss, P.
554 S., Liu, S. M., Middelburg, J. J., Moore, C. M., Nickovic, S., Oschlies, A., Pedersen, T., Prospero,
555 J., Schlitzer, R., Seitzinger, S., Sorensen, L. L., Uematsu, M., Ulloa, O., Voss, M., Ward, B., and
556 Zamora, L.: Impacts of Atmospheric Anthropogenic Nitrogen on the Open Ocean, *Science*, 320, 893-
557 897, <https://doi.org/10.1126/science.1150369>, 2008.

558 Ellis, R., Jacob, D. J., Sulprizio, M. P., Zhang, L., Holmes, C., Schichtel, B., Blett, T., Porter, E., Pardo,
559 L., and Lynch, J.: Present and future nitrogen deposition to national parks in the United States:
560 critical load exceedances, *Atmos. Chem. Phys.*, 13, 9083-9095, 2013.

561 Erismann, J. W., and Draaijers, G.: Deposition to forests in Europe: most important factors influencing
562 dry deposition and models used for generalisation, *Environ. Pollut.*, 124, 379-388, 2003.

563 Eyring, V., Isaksen, I. S., Berntsen, T., Collins, W. J., Corbett, J. J., Endresen, O., Grainger, R. G.,
564 Moldanova, J., Schlager, H., and Stevenson, D. S.: Transport impacts on atmosphere and climate:
565 Shipping, *Atmos. Environ.*, 44, 4735-4771, 2010.

566 Fan, Q., Zhang, Y., Ma, W., Ma, H., Feng, J., Yu, Q., Yang, X., Ng, S. K., Fu, Q., and Chen, L.: Spatial
567 and seasonal dynamics of ship emissions over the Yangtze River Delta and East China Sea and their
568 potential environmental influence, *Environ. Sci. Technol.*, 50, 1322-1329, 2016.

569 Galloway, J. N., Townsend, A. R., Erismann, J. W., Bekunda, M., Cai, Z. C., Freney, J. R., Martinelli, L.

570 A., Seitzinger, S. P., and Sutton, M. A.: Transformation of the nitrogen cycle: Recent trends,
571 questions, and potential solutions, *Science*, 320, 889-892, <https://doi.org/10.1126/science.1136674>,
572 2008.

573 Gao, Y., Leung, L. R., Lu, J., Liu, Y., Huang, M., and Qian, Y.: Robust spring drying in the southwestern
574 U.S. and seasonal migration of wet/dry patterns in a warmer climate, *Geophys. Res. Lett.*, 41, 1745-
575 1751, <https://doi.org/10.1002/2014GL059562>, 2014.

576 Gao, Y., Leung, L. R., Lu, J., and Masato, G.: Persistent cold air outbreaks over North America in a
577 warming climate, *Environ. Res. Lett.*, 10, 044001, 2015.

578 Gao, Y., Lu, J., and Leung, L. R.: Uncertainties in Projecting Future Changes in Atmospheric Rivers and
579 Their Impacts on Heavy Precipitation over Europe, *J. Climate*, 29, 6711-6726,
580 <http://dx.doi.org/10.1175/JCLI-D-16-0088.1>, 2016.

581 Gong, G. C., Shiah, F. K., Liu, K. K., Wen, Y. H., and Liang, M. H.: Spatial and temporal variation of
582 chlorophyll a , primary productivity and chemical hydrography in the southern East China Sea, *Cont.*
583 *Shelf. Res.*, 20, 411-436, 2000.

584 Gong, G. C., Wen, Y. H., Wang, B. W., and Liu, G. J.: Seasonal variation of chlorophyll a concentration,
585 primary production and environmental conditions in the subtropical East China Sea, *Deep-Sea*
586 *Research Part II*, 50, 1219-1236, 2003.

587 Guan, W. J., Xian-Qiang, H. E., Pan, D. L., and Fang, G.: Estimation of ocean primary production by
588 remote sensing in Bohai Sea, Yellow Sea and East China Sea, *J. Fish. China*, 29, 367-372, 2005.

589 Hu, C., Li, D., Chen, C., Ge, J., Muller-Karger, F. E., Liu, J., Yu, F., and He, M. X.: On the recurrent
590 *Ulva prolifera* blooms in the Yellow Sea and East China Sea, *J. Geophys. Res-Oceans*, 115, 2010.

591 Kim, G., Scudlark, J. R., and Church, T. M.: Atmospheric wet deposition of trace elements to Chesapeake
592 and Delaware Bays, *Atmos. Environ.*, 34, 3437-3444, [https://doi.org/10.1016/S1352-](https://doi.org/10.1016/S1352-2310(99)00371-4)
593 [2310\(99\)00371-4](https://doi.org/10.1016/S1352-2310(99)00371-4), 2000.

594 Kim, J. E., Han, Y. J., Kim, P. R., and Holsen, T. M.: Factors influencing atmospheric wet deposition of
595 trace elements in rural Korea, *Atmos. Res.*, 116, 185-194,
596 <https://doi.org/10.1016/j.atmosres.2012.04.013>, 2012.

597 Koga, N., Smith, P., Yeluripati, J. B., Shirato, Y., Kimura, S. D., and Nemoto, M.: Estimating net primary
598 production and annual plant carbon inputs, and modelling future changes in soil carbon stocks in
599 arable farmlands of northern Japan, *Agr. Ecosys. Environ.*, 144, 51-60, 2011.

600 Kryza, M., Werner, M., Dore, A. J., Błaś, M., and Sobik, M.: The role of annual circulation and
601 precipitation on national scale deposition of atmospheric sulphur and nitrogen compounds, *J.*
602 *Environ. Manage.*, 109, 70-79, 2012.

603 Lamarque, J. F., Kiehl, J. T., Brasseur, G. P., Butler, T., Cameron-Smith, P., Collins, W. D., Collins, W.
604 J., Granier, C., Hauglustaine, D., Hess, P. G., Holland, E. A., Horowitz, L., Lawrence, M. G.,
605 McKenna, D., Merilees, P., Prather, M. J., Rasch, P. J., Rotman, D., Shindell, D., and Thornton, P.:
606 Assessing future nitrogen deposition and carbon cycle feedback using a multimodel approach:
607 Analysis of nitrogen deposition, *J. Geophys. Res-Atmos.*, 110,
608 <https://doi.org/10.1029/2005JD005825>, 2005.

609 Lamarque, J. F., Dentener, F., McConnell, J., and Ro, C. U.: Multi-model mean nitrogen and sulfur
610 deposition from the Atmospheric Chemistry and Climate Model Intercomparison Project (ACCMIP):
611 evaluation historical and projected changes, *Atmos. Chem. Phys.*, 13, 7997-8018, 2013a.

612 Lamarque, J. F., Shindell, D. T., Josse, B., Young, P. J., Cionni, I., Eyring, V., Bergmann, D., Cameron-
613 Smith, P., Collins, W. J., Doherty, R., Dalsoren, S., Faluvegi, G., Folberth, G., Ghan, S. J., Horowitz,
614 L. W., Lee, Y. H., MacKenzie, I. A., Nagashima, T., Naik, V., Plummer, D., Righi, M., Rumbold, S.,
615 Schulz, M., Skeie, R. B., Stevenson, D. S., Strode, S., Sudo, K., Szopa, S., Voulgarakis, A., and Zeng,
616 G.: The Atmospheric Chemistry and Climate Model Intercomparison Project (ACCMIP): overview
617 and description of models, simulations and climate diagnostics, *Geosci. Model Dev.*, 6, 179-206,
618 <https://doi.org/10.5194/gmd-6-179-2013>, 2013b.

619 Lauer, A., Eyring, V., Hendricks, J., Jöckel, P., and Lohmann, U.: Global model simulations of the impact
620 of ocean-going ships on aerosols, clouds, and the radiation budget, *Atmos. Chem. Phys.*, 7, 5061-
621 5079, 2007.

622 Laufkötter, C., Vogt, M., Gruber, N., Aitanoguchi, M., Aumont, O., Bopp, L., Buitenhuis, E., Doney, S.
623 C., Dunne, J., and Hashioka, T.: Drivers and uncertainties of future global marine primary production
624 in marine ecosystem models, *Biogeosciences Discussions*, 12, 6955-6984, 2015.

625 Liu, H., Fu, M., Jin, X., Shang, Y., Shindell, D., Faluvegi, G., Shindell, C., and He, K.: Health and climate
626 impacts of ocean-going vessels in East Asia, *Nat. Clim. Change*, 6, 2016.

627 Liu, L., Zhang, X., Xu, W., Liu, X., Lu, X., Chen, D., Zhang, X., Wang, S., and Zhang, W.: Estimation
628 of monthly bulk nitrate deposition in China based on satellite NO₂ measurement by the Ozone
629 Monitoring Instrument, *Remote Sens. Environ.*, 199, 93-106, 2017.

630 Liu, X., Zhang, Y., Han, W., Tang, A., Shen, J., Cui, Z., Vitousek, P., Erisman, J. W., Goulding, K., and
631 Christie, P.: Enhanced nitrogen deposition over China, *Nature*, 494, 459-462, 2013.

632 Luo, X. S., Tang, A. H., Shi, K., Wu, L. H., Li, W. Q., Shi, W. Q., Shi, X. K., Erisman, J. W., Zhang, F.
633 S., and Liu, X. J.: Chinese coastal seas are facing heavy atmospheric nitrogen deposition, *Environ.*
634 *Res. Lett.*, 9, 095007, 2014.

635 Montoya-Mayor, R., Fernandez-Espinosa, A. J., Seijo-Delgado, I., and Ternero-Rodriguez, M.:
636 Determination of soluble ultra-trace metals and metalloids in rainwater and atmospheric deposition
637 fluxes: A 2-year survey and assessment, *Chemosphere*, 92, 882-891,
638 <https://doi.org/10.1016/j.chemosphere.2013.02.044>, 2013.

639 Paerl, and Hans, W.: Coastal eutrophication and harmful algal blooms: Importance of atmospheric
640 deposition and groundwater as "new" nitrogen and other nutrient sources, *Limnol.*
641 *Oceanogr.*, 42, 1154-1165, 1997.

642 Paerl, H. W., Dennis, R. L., and Whitall, D. R.: Atmospheric deposition of nitrogen: Implications for
643 nutrient over-enrichment of coastal waters, *Estuaries*, 25, 677-693, 2002.

644 Price, C., Penner, J., and Prather, M.: NO_x from lightning 1. Global distribution based on lightning
645 physics, *J. Geophys. Res-Atmos.*, 102, 5929-5941, 1997.

646 Qi, J. H., Shi, J. H., Gao, H. W., and Sun, Z.: Atmospheric dry and wet deposition of nitrogen species
647 and its implication for primary productivity in coastal region of the Yellow Sea, China, *Atmos.*
648 *Environ.*, 81, 600-608, 2013.

649 Reay, D. S., Nedwell, D. B., Priddle, J., and Ellis-Evans, J. C.: Temperature dependence of inorganic
650 nitrogen uptake: reduced affinity for nitrate at suboptimal temperatures in both algae and bacteria,
651 *Appl. Environ. Microb.*, 65, 2577-2584, 1999.

652 Reichler, T., and Kim, J.: How well do coupled models simulate today's climate?, *B. Am. Meteorol. Soc.*,
653 89, 303-311, <https://doi.org/10.1175/Bams-89-3-303>, 2008.

654 Shindell, D. T., Lamarque, J. F., Schulz, M., Flanner, M., Jiao, C., Chin, M., Young, P. J., Lee, Y. H.,
655 Rotstayn, L., Mahowald, N., Milly, G., Faluvegi, G., Balkanski, Y., Collins, W. J., Conley, A. J.,
656 Dalsoren, S., Easter, R., Ghan, S., Horowitz, L., Liu, X., Myhre, G., Nagashima, T., Naik, V.,
657 Rumbold, S. T., Skeie, R., Sudo, K., Szopa, S., Takemura, T., Voulgarakis, A., Yoon, J. H., and Lo,
658 F.: Radiative forcing in the ACCMIP historical and future climate simulations, *Atmos. Chem. Phys.*,
659 13, 2939-2974, <https://doi.org/10.5194/acp-13-2939-2013>, 2013.

660 Son, S., Campbell, J., Dowell, M., Yoo, S., and Noh, J.: Primary production in the Yellow Sea determined
661 by ocean color remote sensing, *Mar. Ecol-Prog. Ser.*, 303, 91-103, 2005.

662 Steinacher, M., Joos, F., Frölicher, T. L., Bopp, L., Cadule, P., Cocco, V., Doney, S. C., Gehlen, M.,
663 Lindsay, K., and Moore, J. K.: Projected 21st century decrease in marine productivity: a multi-model
664 analysis, *Biogeosciences*, 7, 979-1005, 2010.

665 Steinfeld, J.: Atmospheric Chemistry and Physics: From Air Pollution to Climate Change, *Environ. Sci.*
666 *Policy Sustainable Dev.*, 40, 26-26, 1998.

667 Stevens, C. J., Lind, E. M., Hautier, Y., Harpole, W. S., Borer, E. T., Hobbie, S., Seabloom, E. W., Ladwig,
668 L., Bakker, J. D., Chu, C. J., Collins, S., Davies, K. F., Firn, J., Hillebrand, H., La Pierre, K. J.,
669 MacDougall, A., Melbourne, B., McCulley, R. L., Morgan, J., Orrock, J. L., Prober, S. M., Risch, A.
670 C., Schuetz, M., and Wragg, P. D.: Anthropogenic nitrogen deposition predicts local grassland
671 primary production worldwide, *Ecology*, 96, 1459-1465, 2015.

672 Tett, P., Droop, M. R., and Heaney, S. I.: The Redfield Ratio and Phytoplankton Growth Rate, *J. Mar.*
673 *Biol. Assoc. UK*, 65, 487-504, 1985.

674 Theodosi, C., Markaki, Z., Tselepidis, A., and Mihalopoulos, N.: The significance of atmospheric inputs
675 of soluble and particulate major and trace metals to the eastern Mediterranean seawater, *Mar. Chem.*,
676 120, 154-163, <https://doi.org/10.1016/j.marchem.2010.02.003>, 2010.

677 Van Vuuren, D. P., Edmonds, J., Kainuma, M., Riahi, K., Thomson, A., Hibbard, K., Hurtt, G. C., Kram,
678 T., Krey, V., and Lamarque, J.-F.: The representative concentration pathways: an overview, *Climatic*
679 *Change*, 109, 5, 2011.

680 Vuai, S. A. H., and Tokuyama, A.: Trend of trace metals in precipitation around Okinawa Island, Japan,
681 *Atmos. Res.*, 99, 80-84, <https://doi.org/10.1016/j.atmosres.2010.09.010>, 2011.

682 Wałaszek, K., Kryza, M., and J. Dore, A.: The impact of precipitation on wet deposition of sulphur and
683 nitrogen compounds, *Ecol. Chem. Eng. S.*, 20, 733-745, <https://doi.org/10.2478/eces-2013-0051>,
684 2013.

685 Wang, L., and Chen, W.: A CMIP5 multimodel projection of future temperature, precipitation, and
686 climatological drought in China, *Int. J. Climatol.*, 34, 2059-2078, 2014.

687 Wang, Y., Zhang, Q., He, K., Zhang, Q., and Chai, L.: Sulfate-nitrate-ammonium aerosols over China:
688 response to 2000–2015 emission changes of sulfur dioxide, nitrogen oxides, and ammonia, *Atmos.*
689 *Chem. Phys.*, 13, 2635-2652, 2013.

690 Xu, W., Liu, L., Cheng, M., Zhao, Y., Zhang, L., Pan, Y., Zhang, X., Gu, B., Li, Y., Zhang, X., Shen, J.,
691 Lu, L., Luo, X., Zhao, Y., Feng, Z., Collett Jr, J. L., Zhang, F., and Liu, X.: Spatial-temporal patterns
692 of inorganic nitrogen air concentrations and deposition in eastern China, *Atmos. Chem. Phys.*, 18,
693 10931-10954, <https://doi.org/10.5194/acp-18-10931-2018>, 2018.

694 Zhang, X. Y., Lu, X. H., Liu, L., Chen, D. M., Zhang, X. M., Liu, X. J., and Zhang, Y.: Dry deposition of
695 NO₂ over China inferred from OMI columnar NO₂ and atmospheric chemistry transport model,
696 *Atmos. Environ.*, 169, 2017.

697 Zhang, Y., Yu, Q., Ma, W., and Chen, L.: Atmospheric deposition of inorganic nitrogen to the eastern
698 China seas and its implications to marine biogeochemistry, *J. Geophys. Res-Atmos.*, 115, 2010.

699